

Nontrivial relaxation dynamics of excitons in high-quality InGaAs/GaAs quantum wells

A. V. Trifonov,¹ S. N. Korotan,¹ A. S. Kurdyubov,¹ I. Ya. Gerlovin,¹ I. V. Ignatiev,¹ Yu. P. Efimov,²
S. A. Eliseev,² V. V. Petrov,² Yu. K. Dolgikh,³ V. V. Ovsyankin,³ and A. V. Kavokin^{1,4}

¹*Spin Optics Laboratory, Saint Petersburg State University, 198504 St. Petersburg, Russia*

²*SPbU Resource Center “Nanophotonics”, Saint Petersburg State University, 198504 St. Petersburg, Russia*

³*Department of Physics, Saint Petersburg State University, 198504 St. Petersburg, Russia*

⁴*Physics and Astronomy School, University of Southampton, Highfield, Southampton, SO171BJ, UK*

(Dated: May 14, 2022)

Photoluminescence (PL) and reflectivity spectra of a high-quality InGaAs/GaAs quantum well structure reveal a series of ultra-narrow peaks attributed to the quantum confined exciton states. The intensity of these peaks decreases as a function of temperature, while the linewidths demonstrate a complex and peculiar behavior. At low pumping the widths of all peaks remain quite narrow (< 0.1 meV) in the whole temperature range studied, 4 – 30 K. At the stronger pumping, the linewidth first increases and then drops down with the temperature rise. Pump-probe experiments show two characteristic time scales in the exciton decay, < 10 ps and 15 – 45 ns, respectively. We interpret all these data by an interplay between the exciton recombination within the light cone, the exciton relaxation from a non-radiative reservoir to the light cone, and the thermal dissociation of the non-radiative excitons. The broadening of the low energy exciton lines is governed by the radiative recombination and scattering with reservoir excitons while for the higher energy states the linewidths are also dependent on the acoustic phonon relaxation processes.

PACS numbers: 78.67.De, 78.55.Cr, 78.47.jg, 71.35.Cc

INTRODUCTION

Excitons in two-dimensional semiconductor structures with quantum wells (QWs) and superlattices may be efficiently coupled to light because of the breaking of the wave vector selection rules along the structure growth direction. Radiative recombination rates of excitons strongly depend on their localization radii. In ideal QWs, the radiative decay of an exciton is possible only if the in-plane component of its wave vector does not exceed one of the photon to be emitted, $K_c = n\omega/c$, where n is the refractive index, ω is the frequency of light. We note that $K_c = 0.03 \text{ nm}^{-1}$ at the exciton resonance frequency in GaAs QWs, which corresponds to an exciton kinetic energy: $E_c = \hbar^2 K_c^2 / (2M_X) = 0.06 \text{ meV}$, which is much lower than the characteristic thermal energy of the system at the liquid helium temperature. Here $M_X = 0.5$ is the exciton mass in units of the free electron mass. Excitons with larger wave vectors do not interact with light. They will be referred to as non-radiative excitons. The oscillator strength of the whole exciton branch is accumulated within its little part (light cone) and the radiative decay rate can reach 10^{11} s^{-1} in GaAs-based structures with QWs.^{1–6} For non-radiative excitons, the dominant mechanism of decay is the phonon-mediated relaxation into the states with small wave vectors followed by the radiative recombination.

An important role of the reservoir of non-radiative excitons was recently recognized for semiconductor microcavities where strong light-matter coupling accelerates the exchange between radiative and non-radiative states.^{7–12} In conventional QW structures, all the dynamic processes are slowed down compared to micro-

cavities, that favors considerable accumulation of non-radiative excitons. The effect of these excitons on the radiative ones may be significant. Non-radiative excitons can be created even at the strictly resonant excitation of the lowest exciton transition if the phonon energy corresponding to the lattice temperature is larger than the critical energy E_c .¹³ The in-plane component of the phonon wave vector, q_{\parallel} , is transferred to the exciton due to the conservation of momentum that results in ejection of this exciton outside the light cone.

For excitons localized by structure defects as well as for excitons scattered by free carriers, phonons and other excitons, the number of atomic oscillators contributing to the exciton oscillator strength is reduced as compared to the free exciton. The radiative decay rate for such excitons may decrease, by up to two orders of magnitude.^{14–16} Besides, structure imperfections may induce additional relaxation processes for radiative as well as for non-radiative excitons. In particular, the defect centers or the QW interface roughness may give rise to the considerable inhomogeneous broadening of exciton resonances and to the non-radiative exciton recombination. For this reason, many attempts were done to study the exciton dynamics in GaAs-based heterostructures of various sample quality.

The exciton dynamics was extensively studied using the photoluminescence (PL) kinetics measurements. Under non-resonant excitation, the PL pulse is characterized by a rise time, $\tau_{\text{rise}} = 10 - 1000 \text{ ps}$, and a decay time, $\tau_{\text{decay}} = 1 - 30 \text{ ns}$, depending on the experimental conditions as well as on the sample design and quality.^{3,5,14,17–24} The theoretical analysis of the data performed in these works and also in Refs.^{2,13,15,25–27} al-

lowed obtaining characteristic rates of processes occurring mainly in the reservoir of non-radiative excitons. It was found that, the characteristic time of exciton formation from free carriers lies in the range from several tens to hundreds of picoseconds.^{19,23,24,28} The exciton thermalization in the reservoir occurs approximately in the same time range.^{13,25,27} These two processes are mainly responsible for the PL rise time in high-quality structures. If radiative excitons are localized due to structure imperfections, their recombination time may become comparable with the time of exciton thermalization in the non-radiative reservoir so that it affects the rise of PL signal.^{15–17} The slowest exciton dynamics process is the scattering of non-radiative excitons into the light cone. This momentum relaxation process is responsible for the PL decay. A large spread of the decay time^{3,5,14,17,18,29,30} is possibly caused by the competition of the momentum relaxation with losses of non-radiative excitons via quenching centers in real structures.

The PL kinetics experiments did not allow to direct measuring the recombination time of radiative excitons in high-quality structures. The first attempts to measure this time at the strictly resonant excitation described in Refs.^{3,5,30,31} were not very successful because of the limited time resolution of the setups used. The recombination as well as the dephasing time for radiative excitons was extensively studied in the pump-probe and four-wave mixing experiments.^{32–38} Results of these studies also reveal large variations of the exciton recombination time in the range 1 — 30 ps, most probably due to the different quality of the investigated structures.

The large spread of experimental data on the exciton relaxation times in structures with QWs points out that the reliable data on characteristic rates of the relaxation processes both for radiative and for non-radiative excitons can be obtained only by the careful selection of high-quality QW structures and in specific experimental conditions.

In this paper, we report on the experimental study of the dynamics of radiative and non-radiative exciton states in a specially designed high-quality heterostructure with a relatively wide InGaAs/GaAs QW of about 95 nm width. The peculiarity of this structure is in the presence of a set of the size-quantized exciton levels, which manifest themselves as the ultra-narrow lines in the PL and reflection spectra. The PL spectra and the kinetics of pump-probe signal were measured under resonant excitation into one of the size-quantized states that allowed us to carefully control the excitation conditions. A comparative analysis of spectral widths of the PL lines and of the results of kinetics measurements has been performed for reliable identification of relaxation processes and extraction of their parameters. In particular, our analysis has shown that the dominant decay process for excitons at the lowest two energy levels is the radiative recombination with a characteristic time shorter than 10 ps.

We have found that the kinetics of pump-probe signal for the lowest exciton state exhibits, besides the fast

component corresponding to the radiative exciton decay, a slow component, whose decay time is longer by three orders of magnitude. The long-lived component of the kinetics is caused by the relaxation of non-radiative excitons from the reservoir to the light cone. We have also identified other relaxation processes in the exciton system under study. In particular, we have found that the increase of excitation density is followed by the enhancement of the exciton-exciton and/or exciton-carrier collisions which broaden exciton lines in the PL spectra. At the same time, the temperature-activated rapid quenching of the PL intensity does not accompanied by any noticeable broadening of exciton lines. We attribute this unusual effect to the thermal dissociation of non-radiative excitons in the reservoir followed by the non-radiative losses of the excitation energy.

I. EXPERIMENTAL DETAILS

We have studied an InGaAs/GaAs quantum well (QW) heterostructure grown by a molecular beam epitaxy at an n-doped GaAs substrate with orientation [001]. The structure was grown at elevated temperature of the substrate of about 550 °C to prevent clusterization of Indium atoms.³⁹ The structure contains a wide InGaAs QW layer with a nominal thickness of about 95 nm and the Indium content of 2%. Besides, it contains a reference narrow QW ($L = 2$ nm) with Indium content of 2% also. There is a gradient of the layer thicknesses of about 10% per cm and the Indium content varies from 1.5 to 2 % in the structure so that the real thickness and potential profile of the wide QW were estimated from spectroscopic data.⁴⁰ The sample was cooled using an optical cryostat with a close cycle of helium cooling. The sample temperature was varied in the range of 4 – 30 K.

The PL was excited by radiation of a tunable continuous-wave Ti:sapphire laser. We excited the QW excitons either quasi-resonantly into one of the size-quantized exciton levels or higher in energy up to the absorption edge of GaAs barriers. The PL was dispersed and detected by a 0.55 m spectrometer equipped with a CCD. The spectral resolution in actual range was about 30 μ eV. Laser spot on the sample was about 50 μ m and excitation power varied in range 2 – 150 μ W. The PL excitation (PLE) spectra were measured using the same setup by means of continuous tuning of the laser wavelength and detecting the PL spectra in the range of several lowest exciton transitions for each excitation wavelength. We would like to note that, due to high quality of the sample, the intensity of PL from two lowest exciton levels dominated over the scattered light of laser tuned to photon energy only one meV above these levels.

Another experimental technique exploited in our study is the pump-probe method. We used pulsed radiation of a femtosecond Ti:sapphire laser, split into the pump and probe beams. The pump beam passed through an acousto-optical tunable filter, which cut out a spectrally

narrow pulses with full width at half maximum of about 0.6 nm corresponding to spectrally-limited pulse duration of about 1.7 ps. The pump wavelength was tuned to excite predominantly the lowest one or two exciton transitions only. The probe pulses were spectrally broad and short, of about 0.1 ps. To detect the time-resolved photo-modulated reflection at different exciton transitions, the spectrum of reflected probe beam was analyzed using a 0.55 m spectrometer equipped with a photodiode.

II. EXPERIMENTAL RESULTS

A. PL, PLE, and reflection spectra at low temperature

The PL and reflectance spectra taken from the same spot on the sample are shown in Fig. 1. The spectra consist of several narrow peaks (resonances), whose positions and widths coincide in both spectra with high accuracy. The absence of any detectable Stokes shift (within experimental error in a few tens of μeV) between the peaks in the PL and reflection spectra indicates high quality of the sample. The energy distance between the resonances approximately corresponds to the energy of size quantization estimated in the framework of the simple model of quantized motion of the exciton as a whole in a wide QW (see, e.g., textbook⁴²). These facts allow us to attribute the observed resonances to optical transitions from/to the size-quantized exciton states.

The resonances in the PL spectrum can be well fitted by a set of Lorentzians, $L(E) = (A/\pi)\delta E/[(E - E_i)^2 + \delta E_i^2]$, superimposed on a background signal. Here E_i is the photon energy for optical transition from size-quantized exciton level i , δE_i is the half width at half maximum (HWHM) of the Lorentzians, A_i is the area under the Lorentzian curve. Because of the gradients of the QW width and of the Indium content, the ratio of integral PL intensities from different exciton levels, A_i/A_1 , slightly depends on the point on the structure surface. Therefore most of the measurements were done at the same spot of the sample.

It should be emphasized that the PL intensity for higher exciton states is comparable with that for the lowest energy state. This feature strongly distinguishes the QW structure under study from those studied by other authors, where the high-energy exciton PL peaks are virtually absent (see, e.g., Ref.⁴³).

In a contrast to the PL spectrum, the integral intensity of the first resonance in the reflection spectrum [see Fig. 1(b)] is considerably larger than that of the second one. Moreover, the maximum reflectivity at the first resonance is about 0.7, not far from unity corresponding to the totally “metallic” reflection. This is the first indication that the radiative decay of these excitons prevails over the nonradiative one.

Additional evidences come from the analysis of widths of exciton lines. As seen in Fig. 1, the spectral broad-

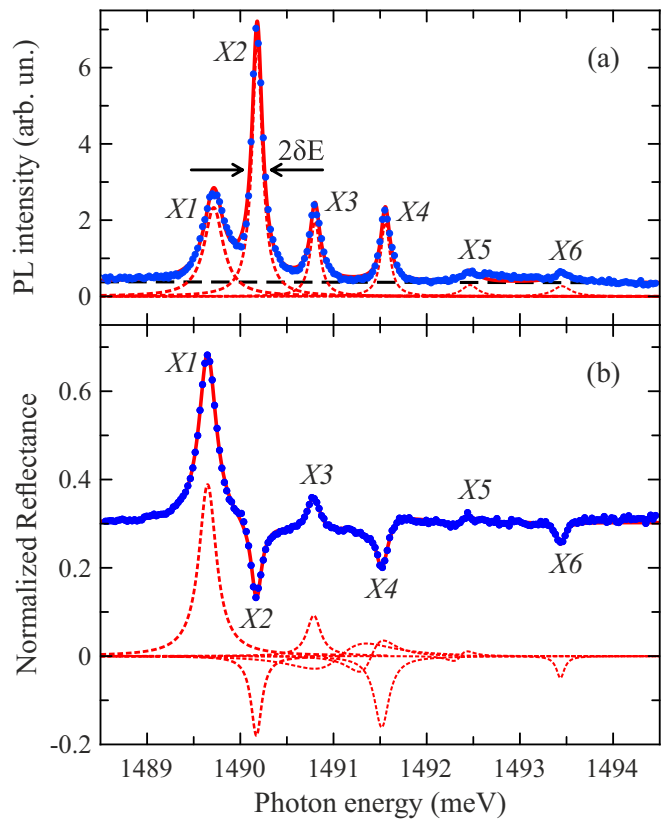


Figure 1. (Color online) PL spectrum of the InGaAs/GaAs QW with nominal width $L = 95$ nm at temperature $T = 4$ K and excitation power $P = 10 \mu\text{W}$ (blue dots). The PL is excited into the $X8$ exciton level. Thin dashed curves are the Lorentzians with parameters for the first four transitions: integral intensity, $A_i = 1080, 1390, 390, 420$ (arb. un.); energy position, $E_i = 1489.71, 1490.18, 1490.80, 1491.56$ (in meV); HWHM, $\delta E_i = 123, 67, 63, 58$ (in μeV), for $i = X1, \dots, X4$, respectively. Notations “ XN ” indicate transitions from the exciton size-quantized levels. The sum of Lorentzians is shown by red solid curve. (b) Reflection spectrum normalized to the excitation intensity (blue dots). Red solid curve shows the phenomenological fit of the resonance features by Lorentzians and their derivatives. Parameters of the first four Lorentzians are: $A_i = 0.139, -0.040, 0.026, -0.049$ (arb. un.); $E_i = 1489.65, 1490.17, 1490.79, 1491.52$ (in meV); $\delta E_i = 113, 70, 91, 96$ (in μeV), for $i = X1 \dots X4$, respectively. The reflectance beyond the spectral features is assumed to be 0.315 typical for reflection from GaAs crystal in this spectral range.⁴¹ The complex shape of the features in reflection spectrum is due to the interference of light waves reflected from the QW layer and from the sample surface.

ening of the lowest transition in both the PL and reflection spectra, $\delta E_1 \sim 0.1$ meV, is extremely small for structures of this type known in literature, see, e.g., Refs.^{18,30,41,44,45} It is also important that the width of higher resonances is considerably smaller than that of the lowest one.

At first glance the latter result is somewhat surprising. Indeed, if the broadening would be caused, e.g., by the

inhomogeneous spread of exciton energies, the width of high-energy resonances would be of the same magnitude or even larger than the ground state linewidth. Moreover, the additional broadening of these peaks might be caused by the relaxation of excitons to the lowest energy level. In fact, only the radiative broadening of the lowest energy exciton resonance is larger than that of the higher energy exciton states.

We estimate the ratio of radiative decay rates of different exciton transitions using a simplified model of size quantization of an exciton in a QW with infinitely high barriers.⁴⁶ The envelope wave functions of the center-of-mass motion of the exciton as a whole are proportional to $\cos(N\pi z/L^*)$ for odd number N of the size quantization exciton level and to $\sin(N\pi z/L^*)$ for even N , where z is the center of mass coordinate along the structure axis. L^* is the effective width of the QW, which is smaller than the real width L by the dead layer width, δL_d .^{47–49} The dead layer width is governed by the exciton Bohr radius, a_B . In our case, $L^* = L - 2\delta L_d \approx 75$ nm assuming that $\delta L_d \approx 0.8a_B = 10$ nm as it is estimated for QWs with a layer thickness of about $6a_B$.⁴⁹

The rate of the radiative transition, γ_{rad} , is proportional to the squared overlap integral of the exciton wave function with the light wave, $F_N^2(k_{ph})$, which, in framework of this model, is:⁴⁶

$$F_N^2(k_{ph}) = \begin{cases} A_N^2 \cos^2(k_{ph}L^*/2) & \text{for odd } N, \\ A_N^2 \sin^2(k_{ph}L^*/2) & \text{for even } N, \end{cases} \quad (1)$$

where

$$A_N = \frac{N\pi/L^*}{\left[(N\pi/L^*)^2 - k_{ph}^2\right]} \sqrt{2/L^*}. \quad (2)$$

Here k_{ph} is the photon wave vector in the QW material. As seen from Eqs. (1, 2), this rate may be strongly different for exciton states with even and odd numbers and gradually decreases with N . For the case of QW under study, equations (1) and (2) give the following transition rates for different size-quantized states normalized to the rate of $X1$ transition: $\gamma_{XN}/\gamma_{X1} = 1, 0.27, 0.043, 0.057, 0.015, 0.025$ for $N = 1, \dots, 6$. Numerical calculations for QWs of similar widths in more accurate models give rise to similar results.^{48,49} The normalized rates obtained qualitatively reproduce the ratio of integral intensities of exciton resonances in the reflectivity spectrum, see Fig. 1(b).⁵⁰

The analysis of the PL spectrum does not provide a direct knowledge of the radiation rates because the intensity of a PL peak depends also on the exciton population, which can be different for different size-quantized states. As one can see in Fig. 1, the integral intensities of the first and second exciton peaks in the PL spectrum are very similar, but this indicates only that the population of the second exciton state is approximately three times larger than that of the first one.

The ratio of line widths in the PL and reflection spectra for the first two exciton transitions gives further support

to the assumption that the main exciton relaxation channel for these transitions is the radiative recombination. The line widths determined from PL spectrum shown in Fig. 1(a) are of about 90 μeV and 40 μeV for the first and second peaks, respectively. This takes into account the spectral resolution of our setup (30 μeV). The ratio of these values is close to the ratio of integrated intensities of the exciton peaks in the reflectivity spectrum discussed above. The exciton relaxation time can be estimated from the linewidth using the relation: $\tau_i = \hbar/(2\delta E_i)$, see, e.g., Ref.,⁴² p. 92. For the first two transitions, the relaxation times are: $\tau_{X1} \approx 4$ ps and $\tau_{X2} \approx 8$ ps. The obtained values are of the same order of magnitude as the radiative recombination time, $\tau_{rad} \sim 10$ ps reported previously for GaAs QWs.^{3,5}

As it seen from the expression (2), the broadening of exciton transitions due to the radiative recombination should rapidly decrease with the increase of the quantum number N . In the PL spectrum [Fig. 1(a)], this tendency is observed only for the first two transitions. Peaks $X3$ and $X4$ have approximately the same HWHM as peak $X2$. At the same time, they have considerably smaller integral intensities than those of the first two peaks. This means that corresponding optical transitions really have smaller radiative probability and their broadening is contributed by additional non-radiative mechanisms.

For a deeper insight into the origin of relaxation processes in the structure, we have measured the PLE spectra of the exciton resonances. Fig. 2(a) shows the spectral dependences of integral intensity for the first four peaks on the photon energy of excitation. The spectra display several remarkable features.⁵¹ The X_{lh} band was identified as the lowest state of the light hole exciton. The degree of circular polarization of PL measured at this resonance has the opposite sign compared to the polarization degree of the heavy hole resonances. This effect is due to different selection rules for respective optical transitions and is well known in literature.⁵² The X_{lh} exciton state is split off from the $X1$ exciton mainly due to the internal strain in the GaAs/InGaAs structure caused by the lattice mismatch of the QW and barriers.

The efficiency of excitation of all the resonances is synchronously changed with the photon energy increase up to the energy of the transition X_{lh} . However, above this transition, the lowest exciton state ($X1$) is populated more efficiently than other states, so that the relative intensity of the corresponding exciton resonance increases. This is an indication that one more relaxation mechanism is “switched on” in this spectral range of excitation. Its possible origin will be discussed in Section III.

Fig. 2(b) shows the dependence of HWHM of the first four exciton peaks on the excitation photon energy. The HWHM were obtained by Lorentzian fitting of the PL spectra measured at each excitation energy. The excitation energy was scanned with small step of about 0.05 meV. As one can see from the figure, the peak broadening noticeably increases above the X_{lh} transition. A particularly strong increase of HWHM is observed for the

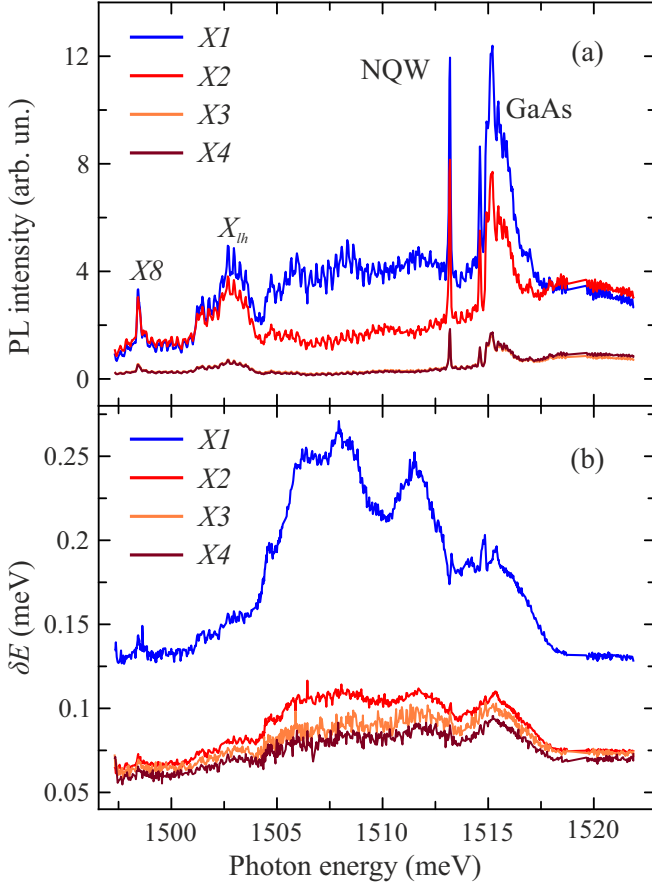


Figure 2. (Color online) PLE spectra for resonances $X1, \dots, X4$. Legends show identification of separate maxima: $X8$ is the eighth size-quantized level of the heavy-hole exciton; X_{lh} is the lowest state of the light-hole exciton; “NQW” is the lowest state of the heavy-hole exciton in the narrow QW; “GaAs” is the exciton in GaAs barriers. (b) HWHM of the resonances as functions of excitation energy. Excitation power $P = 20 \mu\text{W}$.

first resonance that also indicates an additional mechanism of the broadening, which switches on at these photon excitation energies.

B. Temperature and pump power dependences of the exciton resonances

The experimental data discussed in the previous section have been obtained at low temperature (4 K) and low excitation power (10 – 20 μW). In this case the phonon-mediated relaxation and the exciton-exciton scattering are not very efficient. To investigate the role of phonon-mediated processes, we have studied the temperature variations of PL spectra. The temperature rise has been found to be accompanied by a synchronous decrease of the integral amplitude of all exciton resonances, leading to the approximately 20-fold decrease of the total PL intensity with the temperature increase from 4 to 30 K

(see Fig. 3). The temperature dependence of the total PL intensity can be well approximated by expression:

$$I(T) = \frac{I(0)}{1 + \gamma_x \exp\left(-\frac{E_x}{kT}\right) + \gamma_b \exp\left(-\frac{E_b}{kT}\right)} \quad (3)$$

This expression is derived from the balance equation for the exciton population n_X accounting for the radiative recombination rate γ_r , as well as for two non-radiative processes of thermally-activated dissipation of excitons. In such conditions, the balance equation reads:

$$\frac{dn_X}{dt} = P - [\gamma_r + \gamma_X(T) + \gamma_b(T)] n_X \quad (4)$$

Here P is the rate of optical excitation, and the temperature dependences of the exciton dissipation rates are described by Boltzmann functions:

$$\gamma_i(T) = \gamma_{i0} \exp(-E_i/kT), \quad (5)$$

The value of the first activation energy obtained in the fit, $E_x = 4.5 \text{ meV}$, approximately corresponds to the exciton binding energy. Therefore, we assume that the first temperature-activated process is the exciton dissociation into free carriers. The second energy, $E_b = 16 \text{ meV}$, is significantly smaller than the size quantization energy for excitons in the QW under study (of about 25 meV). It appears that the obtained value of E_b is closer to the band offsets for free electrons and/or holes although the ratio of latter quantities is unknown and has been extensively discussed in literature up to now, see, e.g., Refs. 53–55. This is why we conclude that the second temperature-activated process of PL quenching is the emission of carriers into barrier layers accompanied, possibly, by a radiative recombination in a different spectral range.

Besides the PL quenching, the temperature increase helps establishing thermal equilibrium between occupations of different exciton states. In this case, we could expect a remarkable change of the relative intensities of exciton peaks with temperature. In particular, at low temperatures, when the thermal energy, kT , is smaller than the energy distance between the size-quantized levels, the lowest exciton level should be predominantly occupied. At elevated temperatures, when $kT > E_4 - E_1$, the populations of these levels should be nearly equal. The experimental data, however, show that the relative intensities of different PL lines are almost independent of temperature. This means that the efficiency of thermally activated exciton dissociation and carrier ejection is higher than the phonon-mediated transitions between different exciton levels responsible for the thermal equilibrium. We conclude that the thermal equilibrium in the exciton sub-system is not achieved in this structure in the temperature range of 4 – 30 K.

The widths of exciton lines also reveal a surprising, at first glance, behavior at elevated temperatures. A strong decrease of the PL yield with the temperature increase indicates that the non-radiative exciton relaxation begins to dominate over the radiative one at $T > 15 \text{ K}$, see

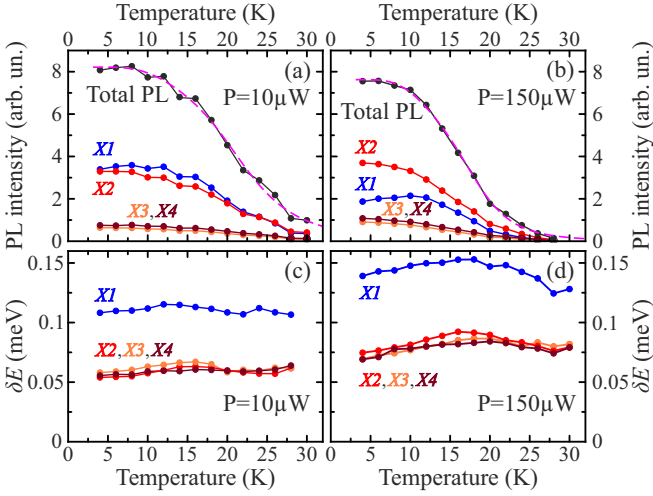


Figure 3. (Color online) Temperature dependencies of integral PL intensities (a, b) and HWHM of different resonances (c, d). Dashed curves in (a) and (b) are the fits by Eqn. 3 with parameters: $\gamma_x = 16$, $\gamma_b = 19500$ for excitation power $P = 10 \mu\text{W}$ in (a); $\gamma_x = 6.4$, $\gamma_b = 3100$ for excitation power $P = 150 \mu\text{W}$ in (b). The activation energies for both excitation powers are: $E_x = 4.5 \text{ meV}$ and $E_b = 16 \text{ meV}$. The dependences were measured at the excitation into the $X6$ transition, whose spectral position was determined at each temperature.

Fig. 3(a, b). If the widths of exciton lines are controlled at low temperature mainly by the radiative processes, the temperature rise should result in line broadening, which is not observed in the experiment. Indeed, as seen in Fig. 3(c), the line widths measured at the low excitation power are almost constant in the temperature range studied within our experimental accuracy.

The increase of the excitation power stronger affects the line widths. Figure 4 shows that it causes an additional line broadening, which is approximately proportional to the square root of the pump power. The additional broadening is a non-monotonic function of temperature: it increases with the temperature rise up to, approximately, $T = 15 \text{ K}$ and then falls down with the further sample heating [comp. Figs 3(c) and (d)]. This behavior is observed for all the excitation powers we used where the additional broadening can be reliably identified.

The low limit of the line broadening observed at the lowest excitation power of $2 \mu\text{W}$ is about 0.1 meV for the resonance $X1$ and 0.05 meV for the $X2$ state, see Fig. 4. These values are comparable with the spectral resolution of our setup, $S \approx 0.03 \text{ meV}$. Using a simplified deconvolution procedure,⁵⁶ we estimated that the “true” HWHM is of about 0.080 meV for the resonance $X1$ and 0.025 meV for the resonance $X2$.

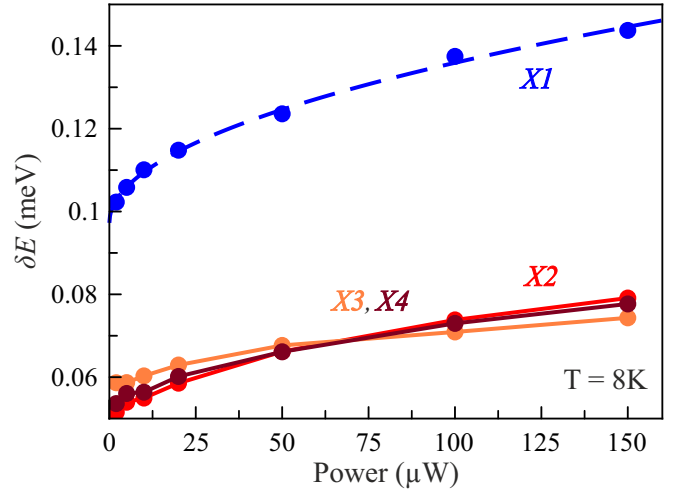


Figure 4. (Color online) Power dependences of HWHM of the resonances measured at $T = 8 \text{ K}$ (symbols). Curves are guides for the eye.

C. Kinetics of exciton states

The most direct knowledge of the exciton relaxation processes can be obtained in kinetic experiments. We have performed pump-probe experiments in the reflection geometry. Figure 5(a) shows the differential reflection signal for two lowest exciton transitions as a function of delay between pump and probe pulses. Similarly to the steady-state reflection [see Fig. 1(b)], the pump-probe signal has different polarities for the first and second exciton transitions. An important peculiarity of the signals is the simultaneous presence of fast and slow components. The slow component is almost unchanged in the time window 0–300 ps.⁵⁷ The fast component rapidly decays with a characteristic time of about 5 ps for the first exciton transition and 8 ps for the second one. These values are close to those obtained from the analysis of line broadening in Sect. II A. This means that the line width is mainly determined by the exciton relaxation and/or recombination processes, whereas the inhomogeneous broadening does not contribute noticeably.

Figure 5(b) shows the spectral dependence of differential reflection measured at the time delay 30 ps when only the slow component persists. The pump pulses were spectrally narrow as shown in the figure. Although the spectral position of the pump pulses has been chosen to excite predominantly the lowest exciton level, the non-zero signal is observed in the wide spectral range up to the light-hole (X_{lh}) exciton transition.

Temperature variations of the pump-probe signal are shown in Fig. 6. One can see that the fast component of the signal undergoes little changes throughout the whole temperature range studied here. In contrast, the slow component strongly changes its amplitude. Moreover, a considerable signal appears at the negative delay where the probe pulse tests the sample before the pump pulse

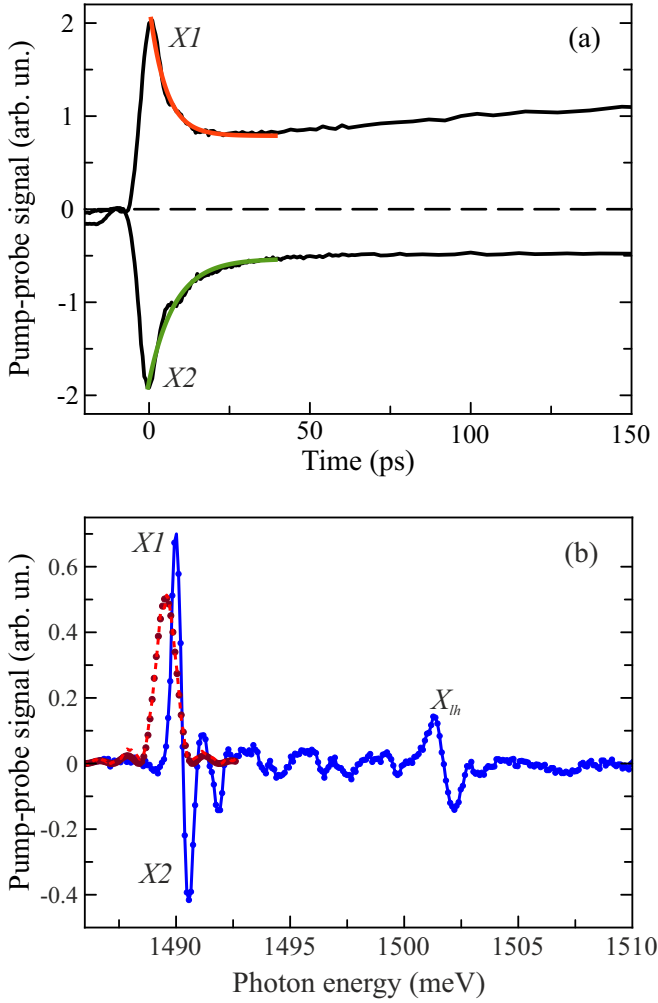


Figure 5. (Color online) Kinetics of pump-probe signal measured at the X1 (upper curve) and X2 resonances at $T = 35$ K. Smooth curves show the fit of the fast component decay of the signal by exponential function, $I(t) = I_0 \exp(-t/\tau)$, with $\tau = 5$ ps and 8 ps for resonances X1 and X2, respectively. (b) Spectral dependence of differential reflection measured at the 30-ps delay after the pump pulse. Dotted curve shows the spectrum of the pump pulse. Dashed curve is a modeling of the pump pulse by function: $I_p(\omega) = I_{p0} (\sin[(\omega - \omega_0)/\delta\omega]/(\omega - \omega_0))^2$ with $\hbar\delta\omega = 0.37$ meV.

arrives. The difference of amplitudes, ΔI , at positive and negative delays is almost unchanged with temperature so that the temperature variations of the pump-probe signal can be described as the variation of a permanent signal (pedestal). The temperature rise from 4 K to 12 K causes a considerable rise of the pedestal. A further increase of temperature gives rise to the rapid drop in the pedestal signal.

The presence of the pump-probe signal at negative delays indicates that the characteristic relaxation time of the slow component, τ_s , exceeds the repetition period of excitation pulses ($T_l = 12.5$ ns). As a result, the detected signal is accumulated from many preced-

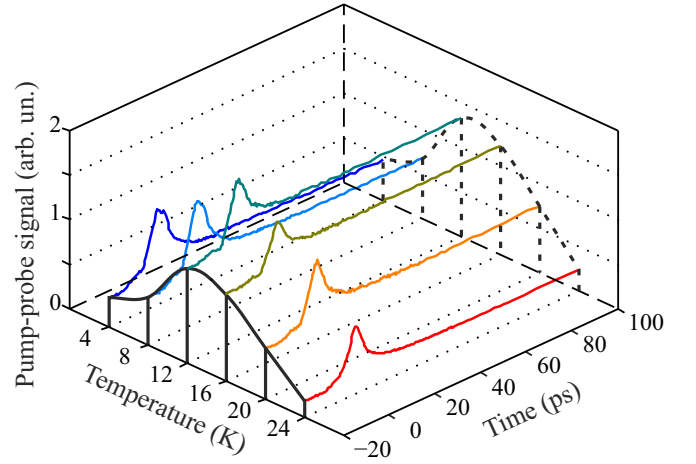


Figure 6. (Color online) Temperature variations of the pump-probe signal for the lowest exciton transition. $P_{exc} = 100 \mu\text{W}$.

ing pump pulses. In the case of exponential decay of the signal, the amplitude of the slow component created by the single preceding pulse is: $I_1 = \Delta I \exp(-T_l/\tau_s)$. The total signal for all the preceding pulses can be easily calculated as a sum of the geometric progression: $I = \Delta I \exp(-T_l/\tau_s)/[1 - \exp(-T_l/\tau_s)]$. This expression allows us to roughly estimate the relaxation time τ_s using the experimentally measured ratio $\Delta I/I$: τ_s increases from 15 ns to 45 ns in the temperature range of 4 – 12 K and rapidly drops with the further temperature increase. At $T > 24$ K, the signal at negative delays is not detectable. This means that the decay time τ_s is shorter than the pulse repetition period T_l .

III. DISCUSSION

The experimental results presented above clearly show that, at low temperature and low excitation power, the structure under study is characterized by extremely narrow widths of exciton resonances and demonstrate zero Stokes shifts between the resonances observed in PL and reflectivity spectra. This is a clear indication of the absence of noticeable inhomogeneous broadening of spectral lines. The line width is controlled solely by the relaxation processes. The larger width of the lowest resonance relative to the second one points out that the predominant contribution to the broadening of these resonances is given by the radiative recombination of excitons.

The absence of any noticeable broadening of the resonances with the temperature rise at quasiresonant excitation with low power (see Fig. 3) is a clear evidence that exciton-phonon interaction does not contribute to the broadening in the temperature range studied. At the same time, the peak width remarkably rises with excitation power (Fig. 4). Because the pump power increase leads to the increase of the exciton density, the observed additional broadening, δE_{X_c} , is most proba-

bly related to exciton-exciton collisions resulting in the phase relaxation of exciton states. The rate of phase relaxation should be proportional to the exciton density and, therefore, to the excitation power. The experiment, however, shows sublinear power dependence, see Fig. 4. We have to assume that the non-linearity is caused by the collision-induced decrease of the radiative recombination rate and of the corresponding broadening, ΔE_r , due to the decrease of the exciton coherence volume. Such effect of phase relaxation on the radiative recombination rate of excitons is theoretically discussed in Refs.^{2,15,26} and experimentally studied in Refs.^{5,33,61} The decrease of radiative broadening partially compensates the collision-induced one so that the total peak broadening, $\Delta E = \Delta E_r + \delta E_{X_c}$ should depend on power sublinearly.²⁶ The linear dependence of integral intensities of exciton peaks on the excitation power (not shown here) evidences that there is no noticeable contribution of other mechanisms, e.g., of non-radiative exciton recombination, to the line broadening in these experimental conditions.

The above-noted increase of relative intensity and width of the first exciton peak at high photon energy of excitation (see Fig. 2) requires a particular attention. These observations point out that the cascade relaxation of photocreated excitons over the size-quantized levels is replaced by the direct carrier relaxation into the lowest exciton level. Indeed, at the excitation above the X_{lh} transition, the probability of resonant excitation with generation of excitons becomes less than the probability of generation of free carriers. The photocreated electrons and holes relax to their ground states where they are bound in excitons. The excitons thus created populate predominantly the lowest energy state, that explains the increased intensity of the $X1$ peak at these excitation conditions. Our assumption about the photocreation of free carriers is further supported by the observation of a strong broadening of the lowest exciton peak. Indeed, according to Refs.,^{23,33} the cross-section of exciton-free-carrier scattering is by an order of magnitude larger than that of the exciton-exciton one. So, the exciton phase relaxation due to exciton-carrier collisions is mainly responsible for the strong broadening of the $X1$ resonance in the case of excitation above the X_{lh} transition.

The temperature dependence of the PL peak intensities and widths (see Fig. 3) appears to be contradictory at the first glance. The temperature increase induces a remarkable decrease of the integral PL that points out to the activation of efficient non-radiative relaxation processes for excitons. The relaxation would seem to be accompanied by a noticeable broadening of exciton peaks, which is not observed in the experiment.

The origin of this effect is related to the temperature dependence of the exciton density in the reservoir. The non-radiative excitons can be efficiently created under non-resonant excitation via one-phonon relaxation as schematically shown in Fig. 7. According to the selection rule, the exciton wave vector in the QW plane should

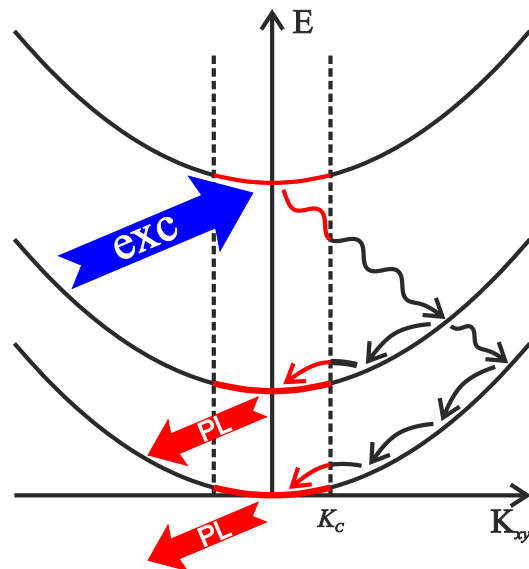


Figure 7. (Color online) A simplified sketch of the processes discussed. Parabolas show the dispersion of the size quantized exciton states along the QW layer. Vertical dashed lines restrict the light cone area of wave vectors. The bold arrows show excitation and PL processes and the wavy arrows show the phonon-mediated exciton relaxation.

to be equal to the projection of the phonon wave vector onto the plane. The energy difference between the nearest exciton levels in our structure is about 0.5 meV or larger. We can estimate the wave vector acquired by an exciton in the course of relaxation via emission of a longitudinal acoustic (LA) phonon. Note that the LA phonons stronger interact with excitons than other acoustic phonons.^{13,25,27} The wave vector of a LA phonon of energy about 0.5 meV in GaAs is 0.07 nm^{-1} , approximately. The light cone is limited by the photon wave vector, $K_c \approx 0.03 \text{ nm}^{-1}$ in GaAs, that is smaller than the phonon wave vector. So, the most part of excitons created by a non-resonant optical excitation should be non-radiative ones.

At low temperature, the main decay channel of non-radiative excitons in high-quality structure is the wave vector relaxation schematically shown in Fig. 7. As a result, non-radiative excitons convert to radiative excitons, and eventually recombine. The rate of this relaxation should be very limited because radiative states are just a small fraction of all states within the exciton band, and the probability for an exciton to be found in one of the radiative states is low. This is why, the lifetime of non-radiative excitons may drastically exceed that of radiative one.

We believe that non-radiative excitons are responsible for the long-lived component of signal in pump-probe experiments, shown in Fig. 5(a). Although the spectral position of excitation pulses is shifted somewhat below the first exciton transition, the finite spectral width of the excitation as well as the presence of some spectral

wings [see Fig. 5(b)] are responsible in this case for the excitation of the high-energy transitions. Exciton relaxation from the states filled in by this way populates the reservoir of non-radiative excitons. The lifetime of the long-lived component, $\tau_{non-rad}$, characterizes the rate of transformation of the non-radiative excitons into radiative ones. At low temperature $\tau_{non-rad} \approx 15$ ns, which is orders of magnitude longer than the lifetime of radiative excitons.

Non-radiative excitons do not directly interact with light. However, as we can see, they give some indirect contribution to reflectance. Because of orthogonality of the wave functions of excitons with different wave vectors, their contribution to the pump-probe signal should not be connected with bleaching of exciton transitions due to phase-space filling considered in Refs.^{58–60} The Coulomb screening effect discussed in these papers is not expected to play a major role at low excitation powers used in our experiments. More probably, the experimentally observed changes in differential reflection are due to the scattering of radiative excitons by non-radiative ones. The scattering results in the broadening of exciton transitions, which is observed, particularly, in the PL spectra at strong pumping, see Fig. 3(d). The broadening changes the reflectivity, which is detected as the pump-probe signal and, correspondingly, as the change of the differential absorption in the vicinity of high-energy exciton transitions, observed experimentally, see Fig. 5(b).

The huge difference in lifetimes of the radiative and non-radiative excitons explains the contradictory temperature behavior of the PL peaks mentioned above. Indeed, the radiative states are mainly populated by the cascade relaxation of photocreated excitons via non-radiative states. Due to the low rate of transformation of non-radiative excitons to radiative excitons, almost all the excitation power is accumulated in the non-radiative exciton reservoir. In particular, the ratio of densities of non-radiative and radiative excitons, $n_{non-rad}/n_{rad} = \tau_{non-rad}/\tau_{rad} \approx 3 \times 10^3$ at $T = 4$ K. The temperature increase triggers the exciton dissociation primarily in this reservoir. The characteristic time of this dissociation process becomes comparable to the lifetime of non-radiative excitons which leads to an efficient depopulation of the reservoir. The depopulation is evidenced by a rapid decrease of the slow component amplitude in the pump-probe signal at $T > 15$ K, see Fig. 5(a). We believe that this is the process responsible for the PL quenching at elevated temperatures. At the same time, the exciton dissociation is still a slow process in comparison with the radiative recombination and, therefore, it cannot have a noticeable effect on the broadening of exciton peaks. This explains the seeming contradiction mentioned above.

The interaction of radiative excitons with non-radiative ones explains the non-monotonic temperature dependence of the PL peak width. The increase of the width when the temperature rises up to 15 K is related to accumulation of non-radiative excitons, which is evidenced in the pump-probe experiments as the increase

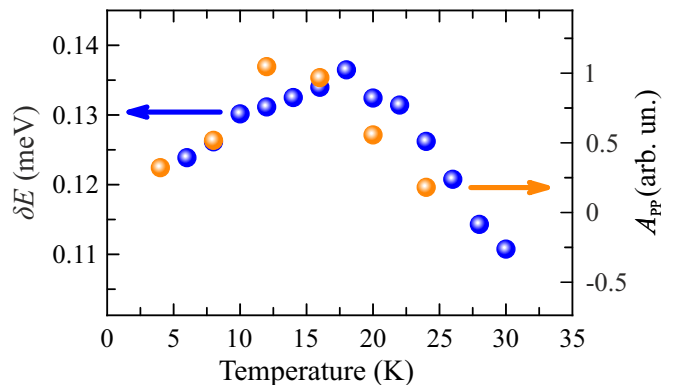


Figure 8. (Color online) Temperature variations of the line broadening for transition X1 measured at excitation power $P = 50 \mu\text{W}$ (blue balls) and of the amplitude of the long-lived component of pump-probe signal (orange balls) shown in Fig. 6. Solid curve shows fit by Eq. (6) with parameters [see Eq. (3)]: $\delta E = 120 \mu\text{eV}$, $\alpha = 3 \mu\text{eV/K}$, $\gamma_x = 14$, $\gamma_b = 6000$. The activation energies are chosen the same as for PL quenching (see Fig. 3).

of the amplitude of long-lived component of the signal (see Fig. 6). The accumulation is caused by the increase of the average kinetic energy and, consequently, of the average wave vector of the non-radiative excitons with the temperature increase. As a result, the exciton relaxation to the light cone is slowed down and their lifetime increases. A simple theoretical analysis predicts a linear temperature dependence of the lifetime and, hence, the density of non-radiative excitons in QWs.^{4,14,62} At higher temperatures, the thermo-activated dissociation of non-radiative excitons reduces their density and, consequently, diminishes the additional broadening of exciton peaks. Figure 8 shows that the peak width and the amplitude of the long lived component exhibit likewise temperature dependencies. This confirms that non-radiative excitons strongly affect both broadening and amplitude. The temperature dependence of δE can be approximated by a function

$$\delta E(T) = \delta E_0 + \alpha T \times I(T), \quad (6)$$

where $I(T)$ is given by Eq. (3).

IV. CONCLUSION

The analysis of PL spectra and relaxation kinetics of size-quantized exciton states in a high-quality wide QW structure allowed us to obtain a valuable information about the most important relaxation processes in this system. Extremely narrow widths of spectral lines and the absence of any Stokes shift between the resonances observed in the PL and reflectivity spectra indicate a high quality of the structure. Our experiments show that, because of the negligibly low density of defects, the most efficient process of exciton decay at low tempera-

tures and low excitation powers is the radiative recombination. This process is responsible for the broadening of the low-energy exciton peaks. The rate of radiative recombination for the higher energy exciton states is reduced. This is why the phonon-mediated relaxation of excitons from higher to lower energy states strongly affects the line broadening. The relaxation process is additionally favored for higher energy states since the density of acoustic phonon states increases as a function of energy.

Our study shows that the kinetics of radiative excitons is strongly affected by the long-lived reservoir of non-radiative excitons whose wave vectors lie outside the light cone. In particular, the reservoir manifests itself in the long-lived component of the pump-probe signal. The lifetime of this component is in three order of magnitude larger than the radiative decay time. It is governed by slow relaxation of non-radiative excitons into the radiative states. At low temperature, the slow relaxation does not lead to a reduction of the PL yield, as non-radiative recombination processes in the reservoir are inefficient in high-quality QWs. The temperature increase up to 30 K results in the strong decrease of exciton PL intensity with no noticeable broadening of the exciton lines. The origin of this unusual effect is in the thermal dissoci-

ation of non-radiative excitons in the reservoir. The dissociation rate is comparable to that of exciton relaxation from non-radiative to radiative states but it is drastically lower than the recombination rate of radiative excitons, which governs the widths of exciton lines. The reservoir of non-radiative excitons also affects the exciton PL spectra. In particular, the scattering of radiative excitons by non-radiative ones at high pumping intensity results in a supplementary broadening of the PL lines.

ACKNOWLEDGMENTS

The authors thank M. M. Glazov and K. V. Kavokin for fruitful discussions. Financial support from the Russian Ministry of Science and Education (contract no. 11.G34.31.0067), SPbU (grants No. 11.38.213.2014) and the Skolkovo Institute of Science and Technology (in the framework of the SkolTech/MIT Initiative) is acknowledged. The authors also thank the SPbU Resource Center “Nanophotonics” (photon.spbu.ru) for the sample studied in present work. A. V. Kavokin acknowledges the support from EPSRC Established Career Fellowship.

-
- ¹ E.I. Rashba, *Fiz. Tverd. Tela (Leningrad)* **4**, 1029 (1962) [*Sov. Phys. Solid State* **4**, 759 (1962)].
 - ² Eiichi Hanamura, *Phys. Rev. B* **38**, 1228 (1988).
 - ³ B. Deveaud, F. Cl  rot, N. Roy, K. Satzke, B. Sermage, and D. S. Katzer, *Phys. Rev. Lett.* **67**, 2355 (1991).
 - ⁴ L.C. Andreani, F. Tassone, F. Bassani, *Solid State Commun.* **77**, 641, (1991).
 - ⁵ A. Vinattieri, Jagdeep Shah, T. C. Damen, D. S. Kim, L. N. Pfeiffer, M. Z. Maialle, and L. J. Sham, *Phys. Rev. B* **50**, 10868 (1994).
 - ⁶ S. W. Koch, M. Kira, G. Khitrova, and H. M. Gibbs, *Nature Mat.* **5**, 523 (2006).
 - ⁷ D. V. Vishnevsky, D. D. Solnyshkov, N. A. Gippius, and G. Malpuech, *Phys. Rev. B* **85**, 155328 (2012).
 - ⁸ M. Wouters, T. K. Para  so, Y. L  ger, R. Cerna, F. Morier-Genoud, M. T. Portella-Oberli, and B. Deveaud-Pl  dran, *Phys. Rev. B* **87**, 045303 (2013).
 - ⁹ M. De Giorgi, D. Ballarini, P. Cazzato, G. Deligeorgis, S. I. Tsintzos, Z. Hatzopoulos, P. G. Savvidis, G. Gigli, F. P. Laussy, and D. Sanvitto, *Phys. Rev. Lett.* **112**, 113602 (2014).
 - ¹⁰ S. S. Demirchyan, I. Yu. Chestnov, A. P. Alodjants, M. M. Glazov, and A. V. Kavokin, *Phys. Rev. Lett.* **112**, 196403 (2014).
 - ¹¹ H. Haug, T. D. Doan, and D. B. Tran Thoai, *Phys. Rev. B* **89**, 155302 (2014).
 - ¹² V. V. Belykh and D. N. Sobyenin, *Phys. Rev. B* **89**, 245312 (2014).
 - ¹³ C. Piermarocchi, F. Tassone, V. Savona, A. Quattropani, and P. Schwendimann, *Phys. Rev. B* **53**, 15834 (1996).
 - ¹⁴ J. Feldmann, G. Peter, E. O. Gobel, P. Dawson, K. Moore, C. Foxon, and R. J. Elliott, *Phys. Rev. Lett.* **59**, 2337 (1987).
 - ¹⁵ D. S. Citrin, *Phys. Rev. B* **47**, 3832 (1993).
 - ¹⁶ A. V. Kavokin, *Phys. Rev. B* **50**, 8000 (1994).
 - ¹⁷ T. C. Damen, Jagdeep Shah, D. Y. Oberli, D. S. Chemla, J. E. Cunningham, and J. M. Kuo, *Phys. Rev. B* **42**, 7434 (1990).
 - ¹⁸ Vivek Srinivas, John Hryniewicz, Yung Jui Chen, and Colin E. C. Wood, *Phys. Rev. B* **46**, 10193 (1992).
 - ¹⁹ J. Szczytko, L. Kappei, J. Berney, F. Morier-Genoud, M.T. Portella-Oberli, and B. Deveaud, *Phys. Rev. Lett.* **93**, 137401 (2004).
 - ²⁰ Ph. Roussignol, C. Delalande, A. Vinattieri, L. Carraresi, and M. Colocci, *Phys. Rev. B* **45**, 6965 (1992).
 - ²¹ L. Kappei, J. Szczytko, F. Morier-Genoud, and B. Deveaud, *Phys. Rev. Lett.* **94**, 147403 (2005).
 - ²² B. Deveaud, L. Kappei, J. Berney, F. Morier-Genoud, M.T. Portella-Oberli, J. Szczytko, and C. Piermarocchi, *Chem. Phys.* **318**, 104 (2005).
 - ²³ D. Bajoni, P. Senellart, M. Perrin, A. Lemait  re, B. Sermage, and J. Bloch, *phys. stat. sol. (b)* **243**, 2384 (2006).
 - ²⁴ M. T. Portella-Oberli, J. Berney, L. Kappei, F. Morier-Genoud, J. Szczytko, and B. Deveaud-Pl  dran, *Phys. Rev. Lett.* **102**, 096402 (2009).
 - ²⁵ P. K. Basu and Partha Ray, *Phys. Rev. B* **45**, 1907 (1992).
 - ²⁶ C. Ciuti, V. Savona, C. Piermarocchi, A. Quattropani, and P. Schwendimann, *Phys. Rev. B* **58**, 7926 (1998).
 - ²⁷ A. L. Ivanov, P. B. Littlewood, and H. Haug, *Phys. Rev. B* **59**, 5032 (1999).
 - ²⁸ C. Piermarocchi, V. Savona, A. Quattropani, P. Schwendimann, and F. Tassone, *phys. stat. sol. (a)* **164**, 221 (1997).
 - ²⁹ M. Gurioli, A. Vinattieri, M. Colocci, C. Deparis, J. Massies, G. Neu, A. Bosacchi, and S. Franchi, *Phys. Rev.*

- B **44**, 3115 (1991).
- ³⁰ R. Eccleston, B. F. Feuerbacher, J. Kuhl, W. W. Rühle, and K. Ploog, *Phys. Rev. B* **45**, 11403 (1992).
 - ³¹ G. Finkelstein, V. Umansky, I. Bar-Joseph, V. Ciulin, S. Haacke, J.-D. Ganière, and B. Deveaud, *Phys. Rev. B* **58**, 12637 (1998).
 - ³² L. Schultheis, A. Honold, J. Kuhl, K. Köhler, and C. W. Tu, *Phys. Rev. B* **34**, 9027 (1986).
 - ³³ A. Honold, L. Schultheis, J. Kuhl, and C. W. Tu, *Phys. Rev. B* **40**, 6442 (1989).
 - ³⁴ Dai-Sik Kim, Jagdeep Shah, T. C. Damen, W. Schäfer, F. Jahnke, S. Schmitt-Rink, and K. Köhler, *Phys. Rev. Lett.* **69**, 2725 (1992).
 - ³⁵ R. Duer, I. Shtrichman, D. Gershoni, and E. Ehrenfreund, *Phys. Rev. Lett.* **78**, 3919 (1997).
 - ³⁶ P. Borri, W. Langbein, J. M. Hvam, and F. Martelli, *Phys. Rev. B* **59**, 2215 (1999).
 - ³⁷ D. S. Chemla and Jagdeep Shah, *Nature* **411**, 549 (2001).
 - ³⁸ R. P. Smith, J. K. Wahlstrand, A. C. Funk, R. P. Mirin, S. T. Cundiff, J. T. Steiner, M. Schafer, M. Kira, and S.W. Koch, *Phys. Rev. Lett.* **104**, 247401 (2010).
 - ³⁹ A. Uddin and T. G. Andersson, *J. Appl. Phys.* **65**, 3101 (1989).
 - ⁴⁰ Ph. S. Grigoryev et al. (unpublished).
 - ⁴¹ S.V. Poltavtsev, Yu.P. Efimov, Yu.K. Dolgikh, S.A. Eliseev, V.V. Petrov, V.V. Ovsyankin, *Solid State Commun.* **199**, 47 (2014)
 - ⁴² E. L. Ivchenko, *Optical spectroscopy of semiconductor nanostructures*, Springer (Berlin) 2004, 437 p.
 - ⁴³ A. Tredicucci, Y. Chen, F. Bassani, J. Massies, C. Deparis, G. Neu, *Phys. Rev. B* **47**, 10348 (1993)
 - ⁴⁴ Y.J. Chen, Emil S. Koteles, Johnson Lee, J.Y. Chi, B.S. Elman, *SPIE* **792**, 162 (1987).
 - ⁴⁵ Rohan Singh, Travis M. Autry, Gaël Nardin, Galan Moody, Hebin Li, Klaus Pierz, Mark Bieler, and Steven T. Cundiff, *Phys. Rev. B* **88**, 045304 (2013).
 - ⁴⁶ H. Tuffigo, R. T. Cox, N. Magnea, Y. Merle d'Aubigné, and A. Million, *Phys. Rev. B* **37**, 4310 (1988)
 - ⁴⁷ E. V. Ubyivovk, D. K. Loginov, I. Ya. Gerlovin, Yu. K. Dolgikh, Yu. P. Efimov, S. A. Eliseev, V. V. Petrov, O. F. Vyvenko, A. A. Sitnikova, and D. A. Kirilenko, *Fiz. Tv. Tela* **51**, 1818 (2009) [*Phys. Sol. State* **51**, 1929 (2009)]
 - ⁴⁸ H. C. Schneider, F. Jahnke, S. W. Koch, J. Tignon, T. Hasche, and D. S. Chemla, *Phys. Rev. B* **63**, 045202 (2001)
 - ⁴⁹ D. Schiumarini, N. Tomassini, L. Piloizzi, and A. D'Andrea, *Phys. Rev. B* **82**, 075303 (2010)
 - ⁵⁰ We should note that the magnitudes of exciton resonances in the reflectivity spectrum shown in Fig. 1(b) are affected by the interference of light reflected by a QW with light reflected from the sample surface. In particular, the magnitude of the second resonance (X_2) is slightly reduced due to this effect.
 - ⁵¹ The low magnitude quasiperiodic oscillations of the PL intensity are due to the interference of the excitation laser light reflected from the optical elements of our setup.
 - ⁵² E.L. Ivchenko, G.E. Pikus, B.S. Razbirin, A.I. Starukhin, *Russian ZhETF* **72**, 2230 (1977) [*JETP* **45**, 1172 (1977)]
 - ⁵³ M. J. Joyce, Z. Y. Xu, and M. Gal, *Phys. Rev. B* **44**, 3144 (1991)
 - ⁵⁴ V. I. Zubkov, M. A. Melnik, A. V. Solomonov, and E. O. Tsvelev, F. Bugge, M. Weyers, and G. Tränkle, *Phys. Rev. B* **70**, 075312 (2004)
 - ⁵⁵ Dipankar Biswas, Partha Pratim Bera, Tapas Das, Sid-dhartha Panda, *Materials Sci. Semicond. Processing* **19**, 11 (2014)
 - ⁵⁶ The experimentally measured profile of exciton resonances represents a convolution of a “true” spectral profile and an apparatus function. We approximate the “true” profile by a Lorentzian function. We convolute the experimentally measured apparatus function with Lorentzians of different HWHM and compare the resulting spectra with the observed exciton peaks in order to extract the “true” HWHM.
 - ⁵⁷ A temporal rise of the slow component observed for the transition X_1 is most probably related to the thermalization of non-radiative excitons in the reservoir as discussed e.g., in Refs.^{5,13} The rise time of the PL signal is of order of several ns at $T = 4$ K and shortens with temperature.
 - ⁵⁸ S. Schmitt-Rink, D. S. Chemla, and D. A. B. Miller, *Phys. Rev. B* **32**, 6601 (1985)
 - ⁵⁹ S. Hunsche, K. Leo, H. Kurz, and K. Köhler, *Phys. Rev. B* **49**, 16565 (1994)
 - ⁶⁰ M. Koch, J. Feldmann, E.O. Göbel, P. Thomas, and J. Shah, and K. Köhler, *Phys. Rev. B* **48**, 11480 (1993)
 - ⁶¹ Félix Fernández-Alonso, Marcofabio Righini, Andrea Franco, and Stefano Selci, *Phys. Rev. B* **67**, 165328 (2003)
 - ⁶² In our case of relatively wide QW, the density of states of non-radiative excitons is a step function with steps at the each size-quantized level. Therefore, the temperature dependence of the exciton lifetime deviates from the linear one proposed for two dimensional excitons and tends to approach the $T^{3/2}$ dependence characteristic of the bulk material, see, e.g., D. Rosales et al., *Phys. Rev. B* **88**, 125437 (2013). We use the linear dependence in the fit in Fig. 8 in order to minimize the number of fitting parameters.